J Physiol (2003), **552.2**, *pp.* 611–620

DOI: 10.1113/jphysiol.2003.041574
www.jphysiol.org

Journal of Physiology

Evaluation of the limiting acuity of coincidence detection in nucleus laminaris of the chicken

Hiroshi Kuba, Rei Yamada and Harunori Ohmori

Department of Physiology, Faculty of Medicine, Kyoto University, Kyoto, 606-8501, Japan

The localization of sounds requires the detection of very brief inter-aural time differences (ITDs). In birds, ITDs are first encoded in neurons of the nucleus laminaris (NL) through the precise coincidence of binaural synaptic inputs. We examined the effects of temperature on acuity of coincidence detection in chick NL, by utilizing whole-cell and cell-attached recording techniques in brain slices while applying electrical stimuli bilaterally to axonal projections from the nucleus magnocellularis to NL. The precision of coincidence detection was measured as a time window, corresponding to the time interval that gave the half-maximum spiking probability. Acuity improved with the elevation of recording temperature, and at 40 °C, the avian body temperature, the time window was 0.38 ms. Although all synaptic events were briefer at higher temperature, the duration of EPSPs were equivalent to or faster than that of EPSCs at 40 °C. Activation of low-threshold K^+ currents by a slight membrane depolarization during an EPSP was responsible for this EPSP acceleration. EPSPs were prolonged following inhibition of low-threshold K^+ currents by dendrotoxin (40 nM) or hyperpolarization-activated cation currents by Cs^+ (3 mM). The EPSP time course had a strong positive correlation with the sharpness of coincidence detection. The limiting value of the time window (0.16 ms), calculated from the estimated EPSP time course, was narrow enough to explain the acuity of ITD detection at NL *in vivo*.

(Received 12 February 2003; accepted after revision 1 August 2003; first published online 1 August 2003)
Corresponding author H. Ohmori: Department of Physiology, Faculty of Medicine, Kyoto University, Kyoto, 606-8501, Japan.
Email: ohmori@nbiol.med.kyoto-u.ac.jp

The difference in the arrival time of sound between the two ears (inter-aural time difference, ITD) is a cue for localizing the origin of sound along the horizontal plane (Klumpp & Eady, 1956; Moiseff & Konishi, 1981). In birds, binaural synaptic inputs first converge in the nucleus laminaris (NL), and it is here that ITDs are initially determined (Carr & Konishi, 1990; Overholt *et al.* 1992). The accuracy of ITD detection at NL is extremely high in the barn owl: when measured as a time window corresponding to an ITD giving half-maximum firing probability, the accuracy varied with best frequency of the neuron, reaching 100–200 μs at the best frequency of 3–7 kHz (Carr & Konishi, 1990; Klump, 2000). This sharp tuning of NL neurons to ITD probably contributes to the resolution of ITDs of 3–6 μs, corresponding to a 1–2 deg azimuthal angle, in the barn owl (Knudsen *et al.* 1979; Moiseff & Konishi, 1981; Klump, 2000). However, it is still unexplained how NL neurons can achieve this acuity of ITD detection.

Previously, we utilized brain slice preparations of chicken embryos to show that the accuracy of coincidence detection at NL was improved by the activation of $GABA_A$ receptors (Funabiki *et al.* 1998) and by the development of short-term synaptic depression (Kuba *et al.* 2002*a*). Moreover, the increase of postsynaptic membrane currents improved the coincidence detection after hatching: they are low-threshold (LT) K^+ current and hyperpolarization-activated mixed-cation current (Kuba *et al.* 2002*b*). However, the time window determined in these experiments was still about 1 ms, significantly broader than that observed in single-unit recordings from NL made in other bird species *in vivo* (several hundred microseconds) (Carr & Konishi, 1990; Klump, 2000). This difference might simply indicate a limitation of whole-cell recordings in slice preparations, or may reflect differences among species. Indeed, in the previous studies, the experimental animals were immature (embryonic 16–20 days), and the experiments were conducted at room temperature (20–25 °C) (Funabiki *et al.* 1998; Kuba *et al.* 2002*a*,*b*), substantially lower than avian body temperature (40 °C).

In this paper, we examined the effects of recording temperature, and addressed the question of how mature NL neurons detect the coincidence of bilateral EPSPs with a physiologically significant acuity. The effects of whole-cell recording on the coincidence detection have been determined, using whole-cell and cell-attached patch-recording techniques. Finally, we will discuss the limiting accuracy of coincidence detection that a single NL neuron can attain and the mechanism by which this acuity can be reached.

METHODS

Slice preparations

Animals were kept and used according to the regulations of the Animal Research Committee, Graduate School of Medicine, Kyoto University. Post-hatch chicks (P2–7) were deeply anaesthetized by halothane (Fluothan, Takeda, Japan) before decapitation, and coronal brain slices (200–300 μm) were obtained as described (Kuba *et al.* 2002*b*). NL neurons used were from the regions representing a characteristic frequency of about 1.1–1.8 kHz (Lippe & Rubel, 1985). Slices were mounted on a recording chamber on the stage of an upright microscope, and were continuously perfused with an artificial cerebrospinal fluid (ACSF, concentrations in mM in this and in subsequent solutions: 125 NaCl, 2.5 KCl, 26 $NaHCO_3$, 1.25 NaH_2PO_4, 2 $CaCl_2$, 1 $MgCl_2$ and 17 glucose). The temperature of the recording chamber was directly measured by a thermistor probe and was controlled between 20 and 40 °C by a Peltier system with water cooling (DTC-300, Dia Medical, Tokyo, Japan). The recording chamber was made of aluminum and coated with Teflon, and a cover glass was glued to the bottom with silicone resin in order to facilitate temperature control. Experiments were generally performed at 40 °C, unless otherwise stated. The pH of ACSF was affected by the recording temperature, and was 7.4 at 20 °C, 7.5 at 30 °C, and 7.6 at 40 °C. This difference in pH did not affect EPSPs: neither the amplitude nor the half-amplitude width was altered ($n = 5$, $P > 0.1$, by Student's paired t test) when pH was changed between 7.0 and 7.8 in the bathing solution (135 NaCl, 2.5 KCl, 10 $NaHCO_3$, 2 $CaCl_2$, 1 $MgCl_2$, 17 glucose, 5 Pipes-Na, 5 Hepes-Na and 5 Tris-Cl) at 20 °C.

Electrophysiological recordings

Whole-cell recordings were made with a patch-clamp amplifier (EPC-8, Heka, Lambrecht, Germany) as described (Kuba *et al.* 2002*b*). Patch pipettes were made from thin-walled borosilicate glass capillaries (GC150TF-100, Harvard, USA) and had a resistance of 4–5 MΩ when filled with a KCl-based internal solution (160 KCl, 0.2 EGTA, 10 Hepes-KOH, pH 7.2), unless otherwise stated. A potassium gluconate-based pipette solution (20 KCl, 140 potassium gluconate, 0.2 EGTA, 10 Hepes-KOH, pH 7.2) was used in some experiments (Fig. 6, see legends for details), and ACSF was used for cell-attached recordings (Figs 1 and 6). Pipettes were coated with a silicone resin (Sylgard, Dow Corning Asia, Japan), and were fire polished before use. The electrode capacitance and the series resistance (5–10 MΩ) were estimated and compensated electronically by 60–80 %. The liquid junction potential (3.1–10.0 mV) was corrected after the experiments. $GABA_A$ receptors were blocked by adding 20–40 μM bicuculline (Sigma, USA) in the extracellular medium, unless otherwise stated. In the experiments of Fig. 5, DTX (dendrotoxin-I, Alomone Labs, Jerusalem, Israel) was bath applied. All the chemicals in this study were supplied from Nacalai (Kyoto, Japan).

Electrical stimulation of presynaptic fibres

Electrical stimuli were biphasic square-wave voltage pulses of 0.1–10 V amplitude and 0.05 ms duration, and were applied through bipolar tungsten electrodes. One electrode to stimulate the ipsilateral projections from the nucleus magnocellularis was placed about 50 μm away from the lateral edge of NL. The other electrode to stimulate the contralateral projection fibres was placed about 50 μm away from the medial edge of NL. We have no evidence of 'cross talk' between the bilateral stimulus electrodes, and we observed neither unilaterally evoked EPSPs with multiple peaks nor the block of EPSP generation by the coupling with the other side of stimuli. Absence of cross talk between the bilateral stimuli was previously confirmed in the case of embryonic NL neurons when stimuli were applied through glass electrodes (Funabiki *et al.* 1998). In experiments to measure coincidence detection (Fig. 2), trains of four stimuli at 10 ms inter-stimulus intervals were applied to projection fibres either unilaterally or bilaterally, changing time separation between the two sides (Δt). Δt was defined as being 0 when the firing probability was maximal, and was generally changed with a step of 0.4 ms between ±2 ms at 20 °C, 0.2 ms between ±1 ms at 30 °C, and 0.1 ms between ±0.5 ms at 40 °C. Positive and negative values indicate contralateral-leading and ipsilateral-leading stimuli, respectively. The firing probability, defined as the total number of spikes divided by the total number of stimuli, was calculated at each Δt from 10–30 traces (40–120 stimuli). Unless otherwise mentioned, the stimulus intensity was tuned at the beginning of each experiment and was maintained throughout the experiment. The stimulus intensity was set close to the threshold level so that the unilateral stimuli alone evoked EPSPs but the intensity was not strong enough to generate a spike consistently during a train (Kuba *et al.* 2002*b*). The firing probability from unilateral stimuli ranged from 0 to 0.13 (0.026 ± 0.005, $n = 49$ cells), and a slight reduction of stimulus intensity failed to generate action potentials even with the coincident bilateral stimuli. In *in vitro* experiments performed in slice preparations of the chicken, a strong stimulus is known to broaden the time window (Joseph & Hyson, 1993). Furthermore, the stimuli did not include the component of timing fluctuation related to acoustic jitter (Warchol & Dallos, 1990; Agmon-Snir *et al.* 1998). Therefore, the present stimuli are likely to be optimized to sharpen the coincidence detection.

Estimation of EPSP half-amplitude width from the capacitive transient in cell-attached recording

When we tested the coincidence detection by cell-attached recording, half-amplitude width of the EPSPs was estimated as follows. Under the cell-attached condition, both negative and positive peaks of capacitive current were recorded when unilateral stimulation was given to projections from the nucleus magnocellularis (Fig. 1*Aa*), and the amplitude of these two peaks was enhanced by bilateral stimuli, suggesting a generation of action potentials from EPSPs (Fig. 1*Ab*). Since the capacitive current is given by $C_{mp}dV_m/dt$, where C_{mp} is the membrane capacitance of the cell-attached patch and V_m the membrane potential, the whole-cell recorded EPSP was time-differentiated to compare the time course of the EPSP with that of its time derivative (Fig. 1*B*). The time interval between the negative and the positive peaks of the derivative (indicated by arrows in Fig. 1*Bb*), corresponding respectively to the maximum rate of rise and fall of the EPSP, matched the 60 % amplitude width of the EPSP (indicated by the horizontal line in Fig. 1*Ba*, correlation coefficient $r = 0.98$, $n = 13$ cells, $P < 0.01$). The half-amplitude width of the EPSP (y) similarly demonstrated a strong positive correlation with this time interval (x) (Fig. 1*C*, $y = 1.11x + 0.03$, $r = 0.93$, $n = 13$ cells, $P < 0.01$). Based on this linear relationship obtained from whole-cell recordings, we calculated the half-amplitude width of EPSPs in cell-attached experiments (Fig. 6). In some cases, EPSPs were recorded after the cell-attached experiments by the same patch pipette, and the half-amplitude width of the EPSPs was found to be consistently longer (0.73 ± 0.04 ms) than the estimate from the cell-attached condition (0.54 ± 0.02 ms) ($n = 12$ cells, $P < 0.01$ by Student's paired t test). This was probably because ACSF filled the cell interior. From the cell-attached patches filled with the KCl-based internal medium, we could not record capacitive transients corresponding to the EPSPs.

Data acquisition and analysis

Data were sampled at 10–33 kHz and were analysed as described previously (Kuba *et al.* 2002*b*). Data are given as means ± standard error of the mean (n = number of cells). Statistical significance was tested with Student's unpaired t test, unless otherwise stated. The mEPSCs from 12–279 recordings were ensemble averaged to show the time course by aligning them to the 50 % rise time for each cell. The membrane time constant was measured by injecting small hyperpolarizing currents (0.04–0.09 nA) of 20 ms duration at the resting membrane potential of about –62 mV under current clamp (see Kuba *et al.* 2002*b*). Analysis of action potentials and synaptic responses was made as described previously (Kuba *et al.* 2002*b*). At 40 °C, action potentials were accelerated and became smaller in size (Fig. 2*Ac*). However, they could still be detected, and appeared as a clear inflection during the rising phase of the EPSP.

Limitations and errors in the measurement of EPSC/P time courses

The time courses were compared between the EPSCs recorded with the patch pipette of standard resistance (4–5 MΩ) and those recorded with a larger pipette under the condition of a reduced EPSC size by applying 6-cyano-7-nitroquinoxaline-2,3-dione (CNQX) (Tocris, USA), where the patch pipette resistance was 1.7–1.9 MΩ and the series resistance was 3–4 MΩ, 70 % compensated. CNQX (2 μM) reduced the EPSC from 1.53 ± 0.21 nA to 0.57 ± 0.17 nA at –80 mV; however, the half-amplitude width of EPSCs was unchanged: 0.42 ± 0.03 ms before and 0.43 ± 0.04 ms after CNQX application (40 °C, n = 5, P = 0.43 by Student's paired t test). These half-amplitude widths were essentially the same as those obtained with the standard pipette resistance and the series resistance compensation in this study (0.48 ± 0.01 ms, n = 30) ($P > 0.1$).

The series resistance compensation critically affects the time course of EPSCs and mEPSCs; turning on the compensation to 70 % (the level we usually adopted) accelerated the time course by 19 % for mEPSCs and 16 % for EPSCs over the uncompensated current traces. Further increase in compensation would improve the measurements only slightly. The half-amplitude width of mEPSCs in the NL neuron (0.25 ms at 40 °C) is larger than that reported in somatic synapses of the nucleus magnocellularis (0.17 ms at 34–36 °C in P2–3 chick; recalculated from Fig. 6*A* of Brenowitz & Trussell, 2001). This somewhat slower time course of the mEPSCs might be a consequence of filtering by dendrites in the NL neuron.

The error in the time course of EPSPs was evaluated by estimating the time constant in the electronic cell composed of a series resistance and a parallel array of resistance and capacitance (the time constant was set at 0.48 ms; measured by a current-clamp amplifier, MEZ-8301, Nihon Kohden, Tokyo, Japan). With the fast mode current clamp of the EPC-8, the measured time constant was almost correct (0.48–0.485 ms) as long as the series resistance was less than 5 MΩ, and the time constant was prolonged with a larger series resistance; the error was 6 % at 10 MΩ. Furthermore, the half-amplitude width of EPSPs measured by the current-clamp amplifier (0.58 ± 0.04 ms, n = 16) was not significantly different from ones measured by the fast mode current clamp (0.63 ± 0.03 ms, n = 22) (P = 0.35) at –62 mV utilizing the standard patch pipette at 40 °C. These control experiments indicate that the time courses of EPSCs, mEPSCs and EPSPs were affected by the series resistance and the speed limitation of the fast mode current clamp of the EPC-8; however, the effects were generally small and were statistically insignificant.

RESULTS

Coincidence detection was improved by increased temperature

Coincidence detection was tested with whole-cell recordings at three different temperatures (Fig. 2*A*). In all cases, both contralateral and ipsilateral stimuli alone barely generated action potentials (Fig. 2*A*, unilateral). Action potentials could be generated when bilateral stimuli were applied, and the number of spikes was maximal for coincident stimuli and decreased with broadening of the stimulus time intervals (Δt, see Methods) (Fig. 2*A*, bilateral). The drop-off in firing probability (see Methods) with increasing time interval was sharper at higher temperatures. In Fig. 2*B*, the firing probability of the neurons in Fig. 2*A* was plotted against Δt and shows that the time window to give the half-maximum firing probability was narrowest at

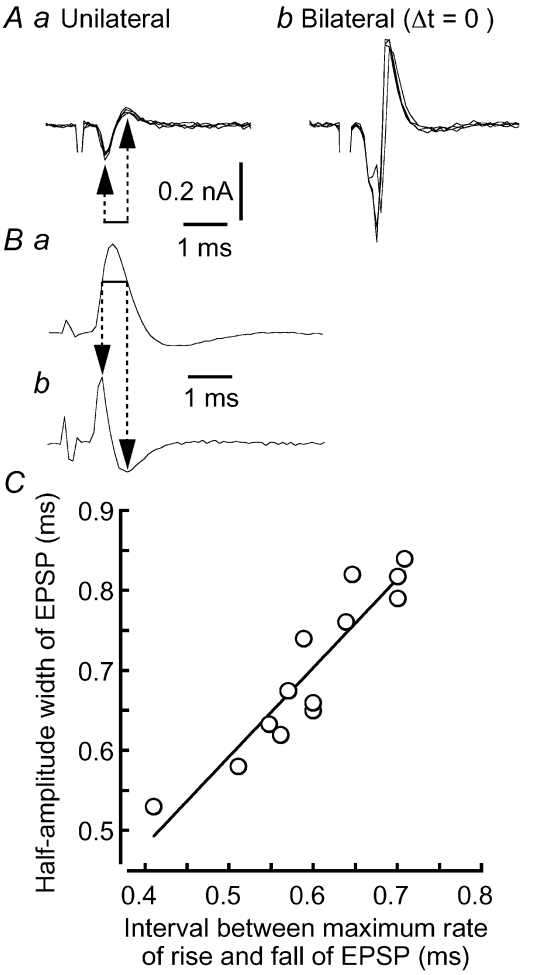

Figure 1. Calculation of EPSP half-amplitude width in cell-attached experiments

A, four superimposed traces when stimuli were applied unilaterally (*a*) and bilaterally (*b*) at coincident timing. *B*, an EPSP recorded under the whole-cell condition (*a*) and its time derivative (*b*). Horizontal line indicates the 60 % amplitude width of the EPSP. *C*, linear relationship between the interval between the maximum rate of rise and fall of EPSPs (arrows in *Bb*) and the half-amplitude width of the EPSPs.

40 °C. When the firing probability was calculated from the population of neurons (Fig. 3*A*), the time window was 0.38 ms at 40 °C ($n = 8$ cells), 0.80 ms at 30 °C ($n = 7$ cells), and 1.4 ms at 20 °C ($n = 6$ cells). At 40 °C, the firing probability decreased by about 60 % between Δt of 0 and ±0.2 ms (shaded area in Fig. 3*A*). An ITD of ±0.2 ms corresponds to a 90 deg azimuthal angle in the auditory space of the chick, due to the effect of the inter-aural canal, which is most effective at sound frequencies less than 1 kHz (Hyson *et al.* 1994). Among the three different recording temperatures, there were no significant differences in the stimulus intensity adopted to test the coincidence detection, the firing probability for the unilateral stimuli, and the firing probability for the bilateral stimuli at coincident timing ($P > 0.1$).

Because whole-cell recordings might affect the excitability of the cell, we next examined the coincidence detection under the cell-attached recording at 40 °C. The time windows were not different between the cell-attached (0.42 ± 0.03 ms, $n = 4$, • in Fig. 6 inset) and the whole-cell recordings (0.37 ± 0.02 ms, $n = 8$, ○ in Fig. 6 inset) ($P = 0.17$). This suggests that the accuracy of coincidence detection was not affected by the recording methods.

Acceleration of the EPSP time course by increased temperature

With the increase in temperature, action potentials were accelerated 3.2-fold between 20 ($n = 6$) and 40 °C ($n = 14$), the half-amplitude width of spikes was shortened to 0.21 ± 0.01 ms ($P < 0.01$), and the threshold of the action potentials became negative by 1.6 mV to –49.5 ± 0.6 mV ($P = 0.13$) at 40 °C. The time course of the EPSPs demonstrated similar acceleration with temperature (Fig. 3*B* inset, amplitudes are scaled). When EPSPs were sampled from the first stimulus during a train where a unilateral stimulus failed to generate an action potential (see the traces demonstrated in Fig. 2*A*), the 10–90 % rise

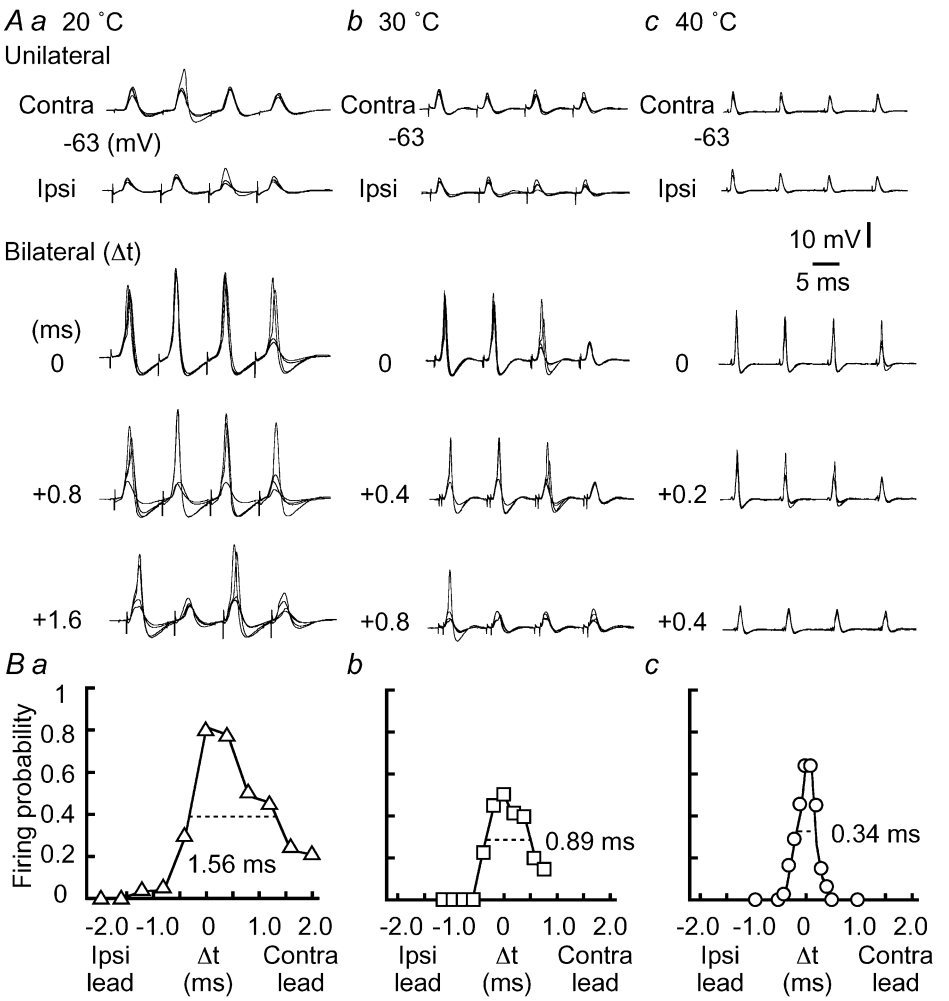

Figure 2. Improved coincidence detection at higher temperatures

A, four superimposed voltage traces in response to unilateral stimuli or bilateral stimuli with three different time intervals between the two sides (Δt in ms, indicated in the figure, see Methods). In *A* and *B*, at 20 °C (*a*), 30 °C (*b*), and 40 °C (*c*). The resting membrane potential is indicated at the left of each trace here and in subsequent figures. *B*, probability of spike generation as a function of Δt calculated from the neurons in *A*. The time window is indicated by the horizontal broken line.

time of the EPSPs (Fig. 3*B*, open column) was shortened 2.7-fold, and the half-amplitude width (filled column), 2.5-fold between 20 and 40 °C. At 40 °C, they were 0.29 ± 0.01 ms and 0.72 ± 0.03 ms ($n = 8$), respectively. However, the amplitudes of the EPSPs were not significantly different: 5.5 ± 0.2 mV ($n = 6$) at 20 °C, 5.1 ± 0.6 mV ($n = 7$) at 30 °C and 5.7 ± 0.5 mV ($n = 8$) at 40 °C ($P > 0.1$). The acceleration of the EPSPs progressed in parallel with the narrowing of the time window for coincidence detection (Fig. 3). This was consistent with the previous report that the decay time constant of EPSPs showed a positive correlation with the time window of coincidence detection in the chicken embryo (Funabiki *et al.* 1998).

EPSCs and mEPSCs were accelerated by increased temperature

The time course of the EPSP is determined both by the EPSC and by postsynaptic membrane properties. EPSCs were evoked by either contralateral or ipsilateral stimuli of threshold intensity: the amplitude of EPSCs was 0.47 ± 0.03 nA ($n = 23$) at 20 °C, 0.78 ± 0.07 nA ($n = 25$) at 30 °C, and 1.02 ± 0.09 nA ($n = 30$) at 40 °C. The increase in temperature accelerated both the EPSCs (thicker traces) and mEPSCs (thinner traces) almost in parallel (Fig. 4*A*). The 10–90 % rise time and the half-amplitude width at 40 °C were 0.19 ± 0.01 ms and 0.48 ± 0.01 ms, respectively, for the EPSCs (Fig. 4*B*, and *C*, filled column, $n = 30$), and 0.085 ± 0.003 ms and 0.25 ± 0.01 ms, respectively for the mEPSCs (Fig. 4*B*, and *C*, open column, $n = 18$). Figure 4*E* plots the histogram to show the distribution of half-amplitude width of mEPSCs recorded at 40 °C ($n = 18$ cells), and the histogram shows a nearly Gaussian distribution (see legends). We measured the half-amplitude width of EPSCs and that of mEPSCs recorded from the same neurons, and the ratio of these measurements was plotted against temperature (Fig. 4*D*). The ratio was 1.86 ± 0.09 ($n = 11$) at 20 °C, 1.66 ± 0.10 ($n = 8$) at 30 °C, and 1.61 ± 0.05 ($n = 13$) at 40 °C, the difference being statistically significant between 20 and 40 °C ($P < 0.05$). This decrease in the ratio might indicate improved synchronization of transmitter release at higher temperatures.

Shaping EPSP time course by the activation of low-threshold K^+ conductance

Time courses of EPSPs (thinner traces) and EPSCs (thicker traces, polarity reversed) recorded from the same neurons are compared in Fig. 5*A*. At lower temperatures of 20–30 °C, both EPSCs and EPSPs were accelerated with the increase in temperature, with decay of the EPSP lagging behind that of the EPSC (Fig. 5*Aa* and *b*). However, at 40 °C, the half-amplitude width of the EPSPs was accelerated to a greater degree than that of the EPSCs (Fig. 5*Ac*). As a consequence, the EPSP was almost superimposed with the EPSC at about the resting potential of −62 mV at 40 °C (Fig. 5*Ac*), and the relative half-amplitude width of EPSPs to that of EPSCs was reduced to 1.21 ± 0.04 ($n = 14$) from 1.41 ± 0.04 ($n = 13$) at 20 °C ($P < 0.01$) (Fig. 5*B*). Between these two recording temperatures, the membrane time constant measured at the resting potential was decreased from 2.2 ± 0.2 ms ($n = 13$) at 20 °C to 0.43 ± 0.02 ms ($n = 40$) at 40 °C ($P < 0.01$). Several ionic currents are activated near the resting potential (Kuba *et al.* 2002*b*), with the contributions of LT K^+ currents being the most significant to the time course of the EPSPs. Application of DTX, known to block the LT K^+ currents (Trussell, 1999), prolonged the EPSP time course about 3-fold compared with the control (Fig. 5*Ae*, and *B*) ($P < 0.01$, $n = 5$), although the time course of EPSCs was not affected ($P = 0.1$, $n = 5$). Consequently, a slight membrane depolarization to –52 mV accelerated the falling phase of the EPSPs, with the time course of EPSPs becoming faster than that of EPSCs (Fig. 5*Ad*) and the ratio of EPSP half-amplitude width to that of the EPSC being less than 1 (0.94 ± 0.04, $n = 10$, Fig. 5*B*). The conductance related to the LT K^+ currents

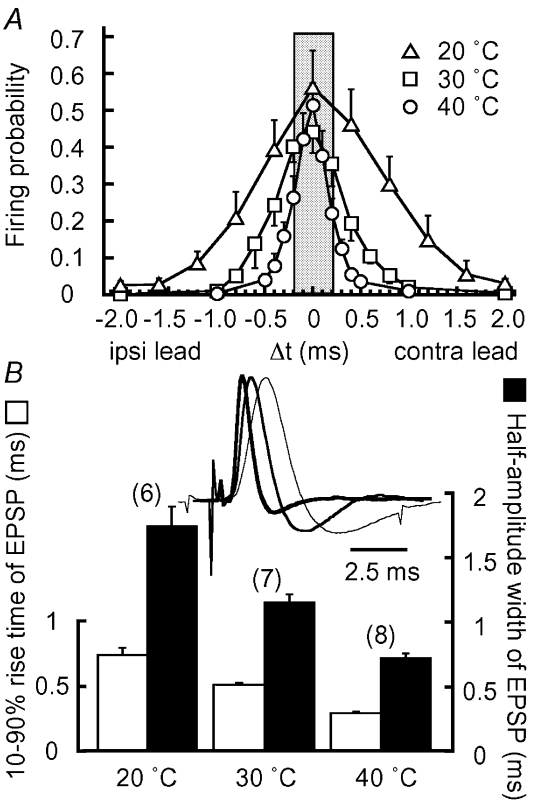

Figure 3. Acceleration of EPSP time course improves coincidence detection

A, firing probabilities calculated from 6 cells at 20 °C (△), 7 cells at 30 °C (□), and 8 cells at 40 °C (○). The grey area indicates the physiological range of ITD in the chick (< 0.2 ms) (Hyson *et al.* 1994). *B*, 10–90 % rise time (open column) and half-amplitude width (filled column) of EPSP from the neurons in *A*. The numbers in parentheses are the numbers of cells, here and in subsequent figures. Inset, subthreshold EPSPs are size-normalized and superimposed to show the progressive acceleration with the increase in temperature; 20 °C (thin trace), 30 °C (intermediate trace), and 40 °C (thick trace).

increased during development in the chicken NL neuron (Kuba *et al.* 2002*b*). Cs^+-sensitive currents, especially the hyperpolarization-activated mixed-cation currents, also increase during development, and contribute to shortening the membrane time constant at about the resting membrane potential (Kuba *et al.* 2002*b*). Application of 3 mM Cs^+ to the bath prolonged the EPSP time course by about 1.3-fold (Fig. 5*Af*), and the relative half-amplitude width of EPSPs to EPSCs was increased to 1.57 ± 0.10 at −62 mV ($n = 8$) ($P < 0.01$ compared with the control, Fig. 5*B*).

EPSP time course determined the time window of coincidence detection

A positive correlation was suggested between the half-amplitude width of EPSPs and the time window of coincidence detection when the recording temperature was changed (Fig. 3). In Fig. 6, the time windows measured under the whole-cell recording condition at temperatures of 20–40 °C in the chick and the chicken embryo (E16–17) (see symbols in Fig. 6 legend) were plotted against the half-amplitude width of EPSP, and the plot showed a strong positive correlation ($r = 0.99$, $n = 42$, $P < 0.01$). As was suggested in Fig. 3, the 10–90 % rise time of the EPSPs similarly showed a positive correlation with the time window ($r = 0.94$, $P < 0.01$), but the amplitude of the EPSPs was not correlated significantly ($r = 0.27$, $P = 0.06$). We further examined the correlation between the time window and the EPSP half-amplitude width in the experiments performed at 40 °C in the chicken, comprising whole-cell (○ and ◇) and cell-attached experiments (• and +) (Fig. 6 inset). There was also a positive correlation between these two parameters. Half-amplitude width of the EPSPs in cell-attached experiments was calculated as described (see Methods and Fig. 1). The regression line between the time window (y) and the EPSP half-amplitude width (x) in the cell-attached experiments ($y = 0.58x$, $r = 0.76$, $n = 23$, $P < 0.01$) was indistinguishable from that in the whole-cell recordings ($y = 0.52x + 0.02$, $r = 0.70$, $n = 13$, $P < 0.01$) ($P > 0.1$). These results indicate that the time course of the EPSPs determines the accuracy of coincidence detection.

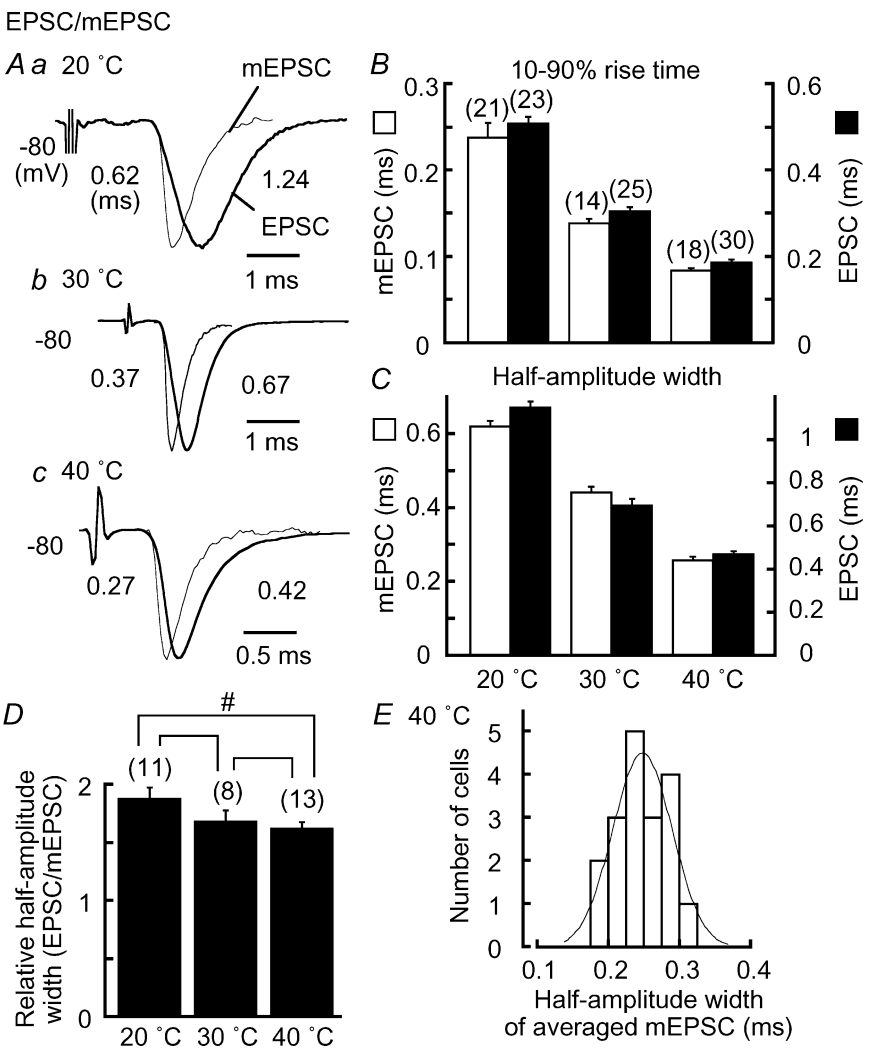

Figure 4. Acceleration of synaptic currents at higher temperatures

A, ensemble averaged mEPSCs (thinner traces) and EPSCs (thicker traces) from the same neurons are size-normalized and superimposed. *a*, at 20 °C; *b*, at 30 °C; *c*, at 40 °C. Half-amplitude width is indicated near each trace (ms). Note the different time scale in *c*. 10–90 % rise time (*B*), and half-amplitude width (*C*) for mEPSCs (open column) and EPSCs (filled column). *D*, half-amplitude width of EPSCs relative to that of mEPSCs. Statistical significance is indicated by # for $P < 0.05$. Brackets without # or ## indicate that differences are statistically insignificant ($P > 0.05$) here and in Fig. 5. *E*, histogram of half-amplitude width of mEPSCs at 40 °C in the chick ($n = 18$ cells). mEPSCs were ensemble averaged in each cell. A Gaussian function was fitted to the histogram with a median of 0.25 ms and standard deviation of 0.04 ms.

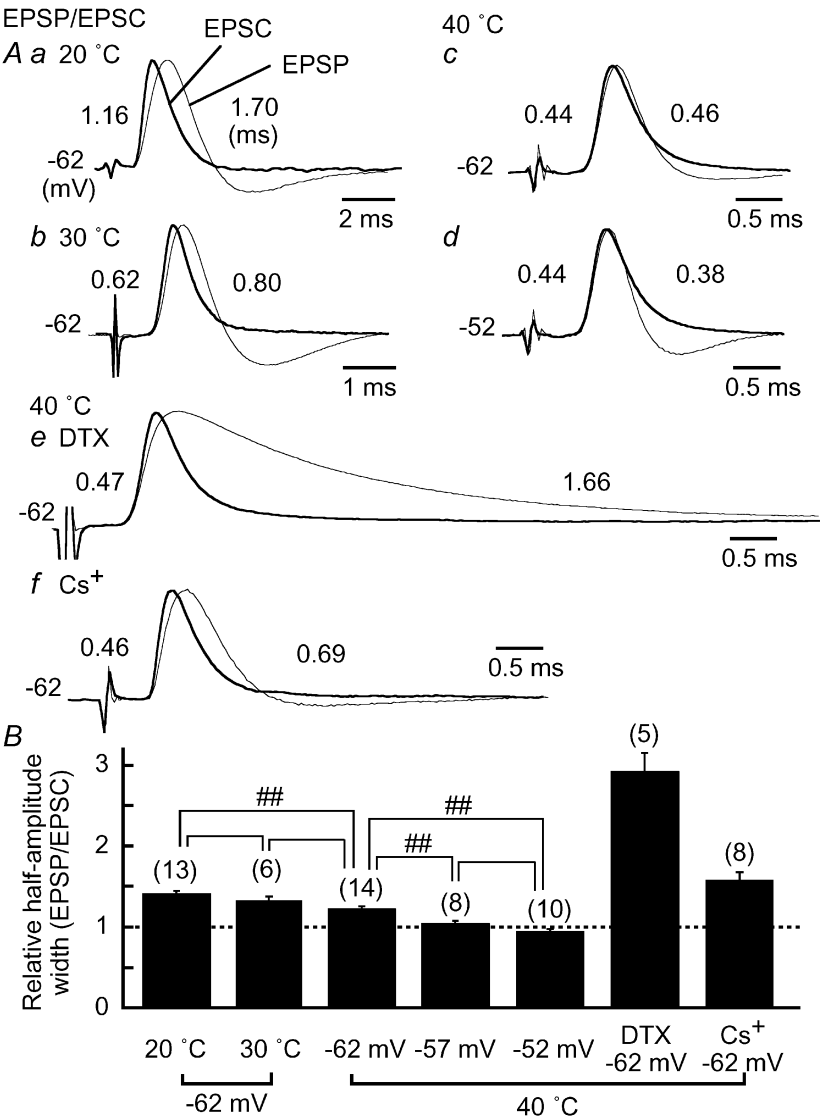

Figure 5. Acceleration of EPSP time course by DTX-sensitive LT K^+ current and by hyperpolarization-activated mixed-cation current

A, EPSP (thinner traces) and EPSC (thicker traces, polarity reversed) from the same neurons were size-normalized and superimposed. EPSPs were recorded at the membrane potential indicated to the left, and EPSCs were recorded at −80 mV. The time course of EPSCs was not different at different holding potentials, at least between −50 and −80 mV. Half-amplitude width is indicated to the left for EPSCs, and to the right for EPSPs. *a*, at 20 °C; *b*, at 30 °C; *c*–*f*, at 40 °C. Note the different time scale in *a* and *b*. *c* and *d* are from the same cell. By depolarization to –52 mV, the amplitude of EPSPs (7.4 ± 0.7 mV) became smaller by 1.1 ± 0.3 mV than at –62 mV ($P < 0.05$ by Student's paired *t* test, $n = 7$). The time course of the EPSPs was prolonged by 40 nM DTX in *e* and by 3 mM CsCl in *f*. The amplitude of the EPSPs was not different before and after drug applications in *e* and *f* ($P > 0.1$), because stimulus intensity was reduced so as not to generate action potentials. *B*, half-amplitude width of EPSPs relative to that of EPSCs. Statistical significance is indicated by ## for $P < 0.01$.

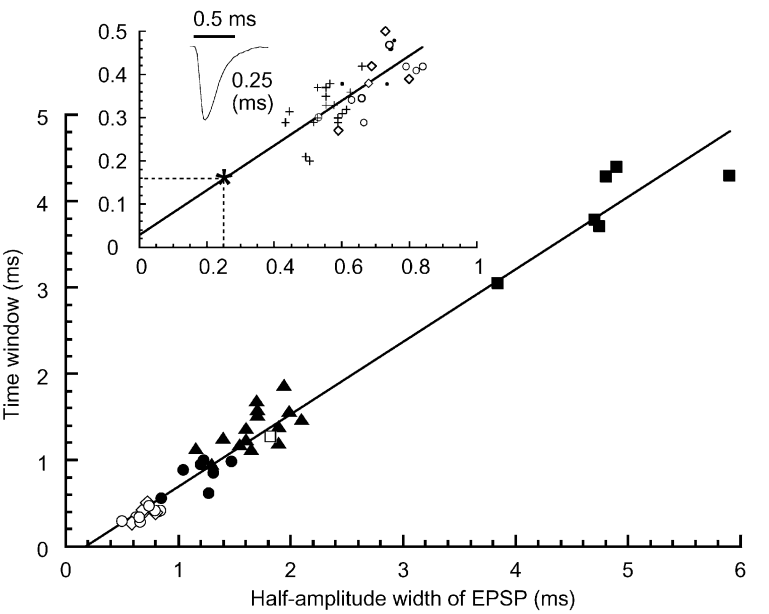

Figure 6. Correlation between the time window and the width of EPSP

Time windows were plotted against the half-amplitude width of EPSP recorded at about −62 mV. Different symbols indicate different experimental conditions: ■, embryo 20–25 °C ($n = 6$); □, embryo 40 °C ($n = 1$); ▲, chick 20–25 °C ($n = 15$); ●, chick 30 °C ($n = 7$); ○, chick 40 °C ($n = 8$); ◇, chick 40 °C without bicuculline using potassium gluconate-based internal solution ($n = 5$). Data from Kuba *et al.* (2002*b*) were included in embryos and chicks at 20–25 °C. Inset, correlation from whole-cell ($n = 13$) and cell-attached experiments ($n = 23$), both performed at 40 °C in the chick. For cell-attached experiments: •, in the presence of bicuculline ($n = 4$) and +, in the absence of bicuculline in the bathing medium ($n = 19$). A trace of mEPSC corresponding to the median of Fig. 4*E* and its half-amplitude width is shown. Time window expected from the mEPSC time course (⋆). The continuous line is the least square fit to the total points at 40 °C in the chick ($y = 0.50x + 0.03$, $r = 0.76$, $n = 36$, $P < 0.01$).

DISCUSSION

These studies have shown that the acuity of coincidence detection was significantly improved by increases in temperature (Figs 2, 3 and 6). Expressed as a time window, the acuity at 40 °C was 0.3–0.4 ms, similar to that reported previously (near 0.5 ms) by extracellular single-unit recordings performed at 34 °C in the same preparation of 7–14 day post-hatch chicks (Joseph & Hyson, 1993). These time windows were comparable to those in other bird species with small heads investigated *in vivo* (budgerigar: approximately 0.3 ms, cited as unpublished data by Amagai in Klump, 2000). Precise coincidence detection was dependent upon the rapid time course of the EPSPs (Figs 3, and 6), which in turn was a function of both the rapid EPSC kinetics (Fig. 4) and the fast postsynaptic membrane responses (Fig. 5). Moreover, the time windows obtained here at 40 °C were not different between whole-cell and cell-attached recordings.

Role of DTX-sensitive LT K^+ currents in coincidence detection

The activation of LT K^+ conductance during the EPSP played a critical role in shortening the EPSP time course. The rapid activation and deactivation of this current could even make the EPSP decay faster than the EPSC (Fig. 5). LT K^+ currents therefore help to improve coincidence detection, a conclusion supported by the observation that block of LT K^+ currents by low doses of 4-aminopyridine (7 μM) broadened the time window of coincidence detection from the control of nearly 1 ms to more than 4 ms in the chick slice preparation at room temperature (Kuba *et al.* 2002*b*). These effects of outward conductance on the coincidence detection had been suggested by current injection experiments performed in slices of chicken embryo (Reyes *et al.* 1996). Consistent with this conclusion, in mammalian medial superior olive (MSO) neurons, the presence of LT K^+ currents improved the signal-to-noise ratio of spike generation in response to synaptic inputs (Smith, 1995; Svirskis *et al.* 2002).

Estimation of the limiting EPSP time course and the accuracy of coincidence detection in NL neurons

In the barn owl, the time window of ITD detection is reported to be as short as 0.1–0.2 ms at characteristic frequencies of 3–7 kHz in the NL neuron by single-unit recordings performed *in vivo* (Carr & Konishi, 1990). This time window of ITD detection is narrower than observations made in NL of other avians (Klump, 2000), and in the MSO of many mammals: dog, 1.2 ms (Goldberg & Brown, 1969); cat, 0.3–2.5 ms (Yin & Chan, 1990); rabbit, 0.5–0.7 ms (Fitzpatrick *et al.* 1997); and gerbil, 0.2–0.4 ms (Brand *et al.* 2002). The barn owl has a superior capability to localize sound origin and can detect a minimum of 1–2 deg changes in the position of the sound source, the minimum audible angle, in the horizontal plane (Knudsen *et al.* 1979). We were curious to know what level of EPSP half-amplitude width might be required in the barn owl NL neuron to calculate ITD with a time window of 0.1–0.2 ms (Carr & Konishi, 1990). Unfortunately, no reports of EPSP or EPSC kinetics are available for the barn owl NL neurons. However, from the regression line in Fig. 6 inset, where experiments were performed at avian body temperature, the EPSP half-amplitude width corresponding to these time windows was expected to be 0.2–0.34 ms, faster than the fastest EPSP in the present study (0.37–0.38 ms, Fig. 5*Ad*). This probable difference of EPSP time course between the chicken and the barn owl might reflect some morphological differences in NL neurons between these two species (Kubke & Carr, 2000), although it is possible that the input resistance of the barn owl NL neurons is much smaller than that of the chicken.

What is the limiting acuity of coincidence detection in the chicken NL? We assumed that the kinetics of EPSCs could approach that of mEPSCs (0.25 ms, Fig. 4*E*) through some increased synchronization of transmitter release (Isaacson & Walmsley, 1995; Borst & Sakmann, 1996; Chuhma & Ohmori, 1998; Kuba *et al.* 2002*b*). In this case, the expected time window was about 0.16 ms (⋆ in Fig. 6 inset), and was comparable to that observed in the NL of the barn owl (Carr & Konishi, 1990). This level of time window could be narrow enough to explain the acuity of coincidence detection reported in *in vivo* studies of other bird species with small heads (Klump, 2000). Further acceleration of the EPSP time course could be expected if the assembly of AMPA receptor subtypes with faster kinetics is made (GluR4 flop with less combination with GluR2 flip)

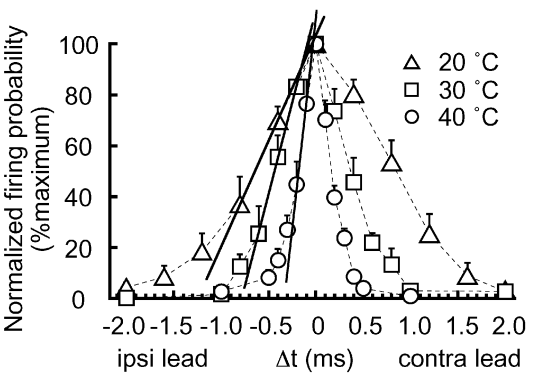

Figure 7. Firing probability as a function of ITD after normalization

Maximum slopes of firing probability as a function of ITD (Δt) were evaluated by re-plotting the firing probability from Fig. 3*A* after normalization was conducted to the maximum (Δt = 0 ms). 20 °C (△, 6 cells), 30 °C (□, 7 cells), and 40 °C (○, 8 cells). The maximum slopes were indicated by continuous lines.

(Mosbacher *et al.* 1994; Geiger *et al.* 1995; Ravindranathan *et al.* 2000), or if more extensive expression of the LT K^+ channel occurs (Trussell, 1999).

Maximum slope of ITD function

We have discussed so far the mechanisms that make the time window of coincidence detection narrow; however, the narrowness of the time window may not be a significant strategy to enable accurate ITD detection. A recent study in gerbils showed that glycinergic IPSPs generated with precise timing shifted the ITD function towards the contralateral direction by approximately 100–300 μs in MSO neurons, with the result that the region of the steepest slope fell in the mid region of the physiological ITD range (Brand *et al.* 2002). Peaks of ITD functions located outside the physiological ITD range are systematically reported in MSO (Goldberg & Brown, 1969; Yin & Chan, 1990; Fitzpatrick *et al.* 1997; Brand *et al.* 2002). These results suggest that the slope of ITD function, rather than its peak or its overall sharpness, is more important in encoding ITDs in mammals (slope coding) (McAlpine *et al.* 2001; Brand *et al.* 2002). Although glycinergic terminals are rare in the chicken NL (Code & Rubel, 1989), the possibility of slope coding has been discussed (Joseph & Hyson, 1993). As shown in Fig. 7, we measured the maximum slope of firing probability as a function of ITD (Δt); the maximum slope between two points was defined as the percentage change of firing probability over 10 μs of time interval. With the increase in temperature, the maximum slope became steeper, being 3.5 at 40 °C, in contrast to 1.5 at 30 °C and 0.9 at 20 °C (Fig. 7). This value was close to that reported for other animals recorded *in vivo* (5–6 in budgerigar NL, calculated from the data by Amagai illustrated in Klump, 2000; 1–3 in gerbil MSO, Brand *et al.* 2002), although the maximum slope was still extremely steep in the barn owl NL (7–15, Carr & Konishi, 1990). The maximum slope of ITD function as well as its narrowness is the dominating feature in the barn owl among all the animals studied, and these features are likely to be essential for the animal to localize the sound source with extreme accuracy. The chicken, as a model animal to understand the neuronal mechanism of auditory coincidence detection, provided substantial data to infer the limiting accuracy of coincidence detection in NL neurons.

REFERENCES

Agmon-Snir H, Carr CE & Rinzel J (1998). The role of dendrites in auditory coincidence detection. *Nature* **393**, 268–272.

Borst JGG & Sakmann B (1996). Calcium influx and transmitter release in a fast CNS synapse. *Nature* **383**, 431–434.

Brand A, Behrend O, Marquardt T, McAlpine D & Grothe B (2002). Precise inhibition is essential for microsecond interaural time difference coding. *Nature* **417**, 543–547.

Brenowitz S & Trussell LO (2001). Maturation of synaptic transmission at end-bulb synapses of the cochlear nucleus. *J Neurosci* **21**, 9487–9498.

Carr CE & Konishi M (1990). A circuit for detection of interaural time differences in the brain stem of the barn owl. *J Neurosci* **10**, 3227–3246.

Chuhma N & Ohmori H (1998). Postnatal development of phase-locked high-fidelity synaptic transmission in the medial nucleus of the trapezoid body of the rat. *J Neurosci* **18**, 512–520.

Code RA & Rubel EW (1989). Glycine-immunoreactivity in the auditory brain stem of the chick. *Hear Res* **40**, 167–172.

Fitzpatrick DC, Batra R, Stanford TR & Kuwada S (1997). A neuronal population code for sound localization. *Nature* **388**, 871–874.

Funabiki K, Koyano K & Ohmori H (1998). The role of GABAergic inputs for coincidence detection in the neurones of nucleus laminaris of the chick. *J Physiol* **508**, 851–869.

Geiger JRP, Melcher T, Koh D-S, Sakmann B, Seeburg PH, Jonas P & Monyer H (1995). Relative abundance of subunit mRNAs determines gating and Ca^{2+}-permeablity of AMPA receptors in principal neurons and interneurons in rat CNS. *Neuron* **15**, 193–204.

Goldberg JM & Brown PB (1969). Response of binaural neurons of dog superior olivary complex to dichotic tonal stimuli: some physiological mechanisms of sound localization. *J Neurophysiol* **32**, 613–636.

Hyson RL, Overholt EM & Lippe WR (1994). Cochlear microphonic measurements of interaural time differences in the chick. *Hear Res* **81**, 109–118.

Isaacson JS & Walmsley B (1995). Counting quanta: direct measurement of transmitter release at a central synapse. *Neuron* **15**, 875–884.

Joseph AW & Hyson RL (1993). Coincidence detection by binaural neurons in the chick brain stem. *J Neurophysiol* **69**, 1197–1211.

Klump GM (2000). Sound localization in birds. In *Comparative Hearing: Birds and Reptiles*, ed. Dooling RJ, Fay RR & Popper AN, pp. 249–307. Springer, New York.

Klumpp RG & Eady HR (1956). Some measurements of interaural time difference thresholds. *J Acoust Soc Am* **28**, 859–860.

Knudsen EI, Blasdel GG & Konishi M (1979). Sound localization by the barn owl (*Tyto alba*) measured with the search coil technique. *J Comp Physiol* **133**, 1–11.

Kuba H, Koyano K & Ohmori H (2002*a*). Synaptic depression improves coincidence detection in the nucleus laminaris in the brainstem slices of the chick embryo. *Eur J Neurosci* **15**, 984–990.

Kuba H, Koyano K & Ohmori H (2002*b*). Development of membrane conductance improves coincidence detection in the nucleus laminaris of the chicken. *J Physiol* **540**, 529–542.

Kubke MF & Carr CE (2000). Development of the auditory brainstem of birds: comparison between barn owls and chickens. *Hear Res* **147**, 1–20.

Lippe W & Rubel EW (1985). Ontogeny of tonotopic organization of brain stem auditory nuclei in the chicken: implications for development of the place principle. *J Comp Neurol* **237**, 273–289.

McAlpine D, Jiang D & Palmer AR (2001). A neural code for low-frequency sound localization in mammals. *Nat Neurosci* **4**, 396–401.

Moiseff A & Konishi M (1981). Neuronal and behavioral sensitivity to binaural time differences in the owl. *J Neurosci* **1**, 40–48.

Mosbacher J, Schoepfer R, Monyer H, Burnashev N, Seeburg PH & Ruppersberg JP (1994). A molecular determinant for submillisecond desensitization in glutamate receptors. *Science* **266**, 1059–1062.

Overholt EM, Rubel EW & Hyson RL (1992). A circuit for coding interaural time differences in the chick brainstem. *J Neurosci* **12**, 1698–1708.

Ravindranathan A, Donevan SD, Sugden SG, Greig A, Rao MS & Parks TN (2000). Contrasting molecular composition and channel properties of AMPA receptors on chick auditory and brainstem motor neurons. *J Physiol* **523**, 667–684.

Reyes AD, Rubel EW & Spain WJ (1996). *In vitro* analysis of optimal stimuli for phase-locking and time-delayed modulation of firing in avian nucleus laminaris neurons. *J Neurosci* **16**, 993–1007.

Smith PH (1995). Structural and functional differences distinguish principal from nonprincipal cells in the guinea pig MSO slice. *J Neurophysiol* **73**, 1653–1667.

Svirskis G, Kotak V, Sanes DH & Rinzel J (2002). Enhancement of signal-to-noise ratio and phase locking for small inputs by a low-threshold outward current in auditory neurons. *J Neurosci* **22**, 11019–11025.

Trussell LO (1999). Synaptic mechanisms for coding timing in auditory neurons. *Annu Rev Physiol* **61**, 477–496.

Warchol ME & Dallos P (1990). Neural coding in the chick cochlear nucleus. *J Comp Physiol A* **166**, 721–734.

Yin TCT & Chan JCK (1990). Interaural time sensitivity in medial superior olive of cat. *J Neurophysiol* **64**, 465–488.

Acknowledgements

We thank the anonymous referee of the Journal for editing English expressions, Professors A. Noma and T. Kaneko for critical comments and valuable suggestions, Drs K. Koyano and T. M. Ishii for discussions and Mr M. Fukao for machining the equipment.